

Detection of Small Pulmonary Nodules on Chest Radiographs: Efficacy of Dual-
Energy Subtraction Technique Using Flat-Panel Detector Chest Radiography

ABSTRACT

AIM:

We investigated the effect of a double-exposure dual-energy subtraction (DES) technique on the performance of radiologists detecting small pulmonary nodules on flat-panel detector (FPD) chest radiographs.

MATERIALS AND METHODS:

Using FPD radiography we obtained 41 sets of chest radiographs from 26 patients with pulmonary nodules measuring ≤ 20 mm and from 15 normal subjects. Each data set included standard- and corresponding DES images. There were 6 non-solid-, 10 part-solid-, and 10 solid nodules. The mean size of the 26 nodules was 15.0 ± 4.8 mm. We performed receiver operating characteristic (ROC) analysis to compare the performance of 8 board-certified radiologists.

RESULTS:

For the 8 radiologists, the mean value of the area under the ROC curve (AUC) without and with DES images was 0.62 ± 0.05 and 0.68 ± 0.05 , respectively; the difference was statistically significant ($p = 0.02$). For part-solid nodules, the difference of the mean AUC value was statistically significant (AUC = 0.61 ± 0.07 vs. 0.69 ± 0.05 ; $p < 0.01$); for non-solid nodules it was not (AUC = 0.62 ± 0.10 vs. 0.61 ± 0.09 ; $p =$

0.73), and for solid nodules it was not ($AUC = 0.75 \pm 0.10$ vs. 0.78 ± 0.08 ; $p = 0.23$).

For nodules with overlapping bone shadows, the difference of the mean AUC value was statistically significant ($p = 0.03$), for nodules without overlapping, it was not ($p = 0.26$).

CONCLUSION:

Use of a double-exposure DES technique at FPD chest radiography significantly improved the diagnostic performance of radiologists detecting small pulmonary nodules.

INTRODUCTION

Chest radiography remains the most widely used imaging technique for the detection of chest diseases because of its low cost, simplicity, and low radiation dose. However, the false-negative rate for the detection of pulmonary nodules is relatively high; it was reported to range from 19 to 72%,^{1,2} and radiography is inferior to low-dose computed tomography (CT) with respect to the detection of small pulmonary nodules.³ The failure to detect pulmonary nodules on chest radiographs has been attributed to their size⁴ and density⁵ and obscuration by structures such as the ribs, clavicles, mediastinum, and pulmonary vessels.⁶ In fact, 82 - 95% of lung cancers missed by radiologists were partly obscured by overlying bones such as the ribs and/or clavicles.⁶

The dual-energy subtraction (DES) technique for chest radiography can remove overlying bone structures to create soft-tissue-selective images^{7,8} and it enhances the visualization of pulmonary nodules overlaid by bones. Consequently, its use may improve the detectability of chest lesions, especially small pulmonary nodules. The DES technique is now available in full-field digital flat-panel detector (FPD) radiography systems that are widely used because of the rapid accessibility of images, improved image quality, and the possibility of reduced radiation exposure.⁹

We investigated the clinical efficacy of a double-exposure DES technique using FPD chest radiography systems in the detection of pulmonary nodules smaller than 20 mm.

MATERIALS AND METHODS

Our study was approved by our institutional review board (IRB); informed consent was obtained from all patients who underwent double-exposure DES radiography. Our IRB also approved the participation of the 8 radiologists in the observer performance test. Informed consent for the observer performance study was obtained from all participants.

Database

Between August 2007 and February 2008, 136 patients underwent double-exposure DES radiography and chest CT for the evaluation of chest diseases in our department. One chest radiologist (K.A.) with 22 years of chest CT experience, who did not participate in the observer performance study, selected chest radiographs based on the following inclusion criteria: (1) DES radiography and chest CT were performed within 14 days, (2) no treatment or biopsy was performed between the 2 procedures, (3) the presence of only one pulmonary nodule without calcification confirmed by CT study, (4) the pulmonary nodules did not exceed 20 mm in the x-y (or transverse) plane on thin-section CT, (5) visibility of the pulmonary nodules on chest radiographs, (6) absence on CT scans of other pleural and parenchymal abnormalities such as

consolidation, diffuse ground glass opacity (GGO), and pulmonary fibrosis. Based on these criteria we identified 26 patients, 11 men and 15 women ranging in age from 40-85 years (mean 62.9 years). The radiologist recorded the location of the nodules on chest radiographs. The same radiologist also selected 15 individuals, 11 men and 4 women ranging in age from 48-64 years (mean 55.5 years) without CT evidence of nodules or other chest diseases. Of the 26 patients with pulmonary nodules, 13 had bronchioloalveolar carcinoma, 9 adenocarcinoma, 1 squamous cell carcinoma, 2 solitary pulmonary metastasis, and 1 had a hamartoma. The histological diagnoses were confirmed at thoracic surgery. The mean size of the pulmonary nodules on CT was 15.0 ± 4.8 mm (range 7.1 - 20.0 mm). The chest radiologist classified the 26 nodules as non-solid- (pure GGO-, n=6), part-solid- (mixed GGO-, n=10) and solid nodules (n=10) according to their internal density.¹⁰ He also classified the nodules into two types i.e. as nodules with and without overlapping bone shadows on chest radiographs. Overlapping was recorded when 50% or more of the nodular area overlapped with ribs and/or clavicles. Of the 26 nodules, 9 (34.6%) did and the other 17 did not overlap.

DES Chest Radiography and Chest CT

DES chest radiographs were obtained using a FPD digital chest system (Revolution XR/d, GE Healthcare, Milwaukee, WI). The detector featured an image size of 41 × 41 cm and a pixel dimension of 0.2 × 0.2 mm. DES images were acquired with a double-exposure technique with 200 ms between the high- (120-kV) and low-energy (60-kV) exposures; standard posteroanterior-, soft-tissue-, and bone images were generated (Fig. 1). The imaging parameters included a 120-kV image acquired at a speed equivalent to approximately 400, and a 60-kV image obtained at a speed setting equivalent to approximately 1000. Speed is representative of the photoreceiver sensitivity of the detector. Our phantom study had shown that the radiation dose for a standard posteroanterior chest radiograph with the FPD system was 97 μGy; it was 168 μGy for double-exposure DES imaging at the above speed settings (unpublished data). The radiation dose at double-exposure DES chest radiography with the FPD system is nearly equal to that of conventional computed- or film-screen radiography systems.⁹

CT imaging was with a 64-detector CT scanner (Brilliance-64, Philips Medical Systems, Cleveland, OH). The scanning parameters were: detector collimation 64 x 0.625 mm, helical pitch 0.673, rotation time 0.5 sec, tube voltage 120 kVp, tube current 250 mAs, and continuous reconstruction at 1.5 mm, and 5 mm slice thickness.

Observer Performance Study

We used a sequential-test method for receiver-operating-characteristic (ROC) analysis to evaluate the diagnostic performance of radiologists detecting small pulmonary nodules on chest images without and with DES images. They were 8 board-certified radiologists with 12 - 22 years of experience (mean 15.6 years). All specialized in body imaging and read chest radiographs regularly. They were allowed to change the level and width of the window on the monitor; reading time was not limited.

All observers used a continuous rating scale and a line-marking method to rate their confidence level by placing marks on a 7-cm-long line on a recording form. The left end of the line indicated complete confidence that the chest radiographs without/with DES images did not reveal a nodule, the right end indicated complete confidence that they did reveal a nodule. Intermediate levels of confidence were indicated by the position of the marks between the 2 line termini, where marks close to the right and left end indicated a greater and lesser degree of confidence, respectively. One author (Y.F.) then measured the distance between the left end of the line and the mark and converted the distance to an ordinal confidence rating ranging from 0 - 100. A continuous rating scale containing a pair of horizontal lines was used in the sequential

test. Observers first recorded their rating of chest radiographs without DES images on the upper line. Subsequently, they recorded their rating of DES images on the lower line. They entered their results for each case on a record form. All observers also recorded the location of detected nodules on record sheets.

First, to become familiarized with the observer study, each observer received training that involved reading images of 5 training cases that were not included in the 41 used in the observer performance study. The observers read the training cases during about 15 min just before the observer performance test. The 5 training cases consisted of 2 patients with- and 3 patients without nodules. The observers were instructed to use the rating scale consistently and uniformly. Before training and test-taking, they were informed that the purpose of the experiment was to evaluate whether the DES technique did, or did not enhance the detection of pulmonary nodules on chest radiographs. No patient information was provided to the observers.

Statistical Analysis

We used ROC analysis to compare the radiologists' performance in detecting pulmonary nodules on chest images acquired without and with the DES technique. A binormal ROC curve was fitted to each radiologist's confidence rating data acquired

under the 2 reading conditions by applying quasi-maximum likelihood estimation.¹¹ A computer program (ROCKIT; Charles E. Metz, University of Chicago, Chicago, IL) was used for obtaining binormal ROC curves from the ordinal-scale rating data.¹¹ The area under the best-fit ROC curve (AUC) plotted in unit squares was calculated for each fitted curve.

The statistical significance of the difference in AUC values between the ROC curves obtained without and with DES images was tested. The paired t-test was performed with a statistical software package (SPSS, version 15.0; SPSS, Chicago, IL), and p values less than 0.05 were considered to indicate statistically significant differences.

RESULTS

We obtained good-quality DES images in all study cases. There were no unacceptable DES images due to misregistration artifacts attributable to cardiac-, respiratory-, and patient motion.

For all pulmonary nodules the AUC values for all 8 observers were higher with than without DES images (Table 1). Analysis of the overall performance of the 8 observers in the detection of pulmonary nodules indicated that the mean AUC values for all observers increased from 0.62 ± 0.05 (without DES images) to 0.68 ± 0.05 (with DES images); the difference was statistically significant ($p = 0.02$) (Fig. 2).

For part-solid nodules ($n=10$) the mean AUC values without and with DES images were 0.61 ± 0.07 and 0.69 ± 0.05 , respectively; the difference was significant ($p < 0.01$). For non-solid nodules ($n=6$), these values were 0.62 ± 0.10 and 0.61 ± 0.09 , respectively and the difference was not significant ($p = 0.73$). For solid nodules ($n=10$), they were 0.75 ± 0.10 and 0.78 ± 0.08 , respectively and the difference was not significant ($p = 0.23$) (Table 2).

For nodules with overlapping bone shadows, the mean AUC values obtained without and with DES images were 0.66 ± 0.05 and 0.72 ± 0.05 , respectively; the

difference was significant ($p = 0.03$) (Table 3). For nodules without overlapping it was not significant ($AUC = 0.58 \pm 0.06$ vs. 0.62 ± 0.06 , respectively; $p = 0.26$).

When an observer correctly identified the location of the nodules and assigned a confidence level of 50 or more, the mean of sensitivity, specificity, accuracy, and positive- and negative predictive value (PPV, NPV) for all observers was 47.6%, 72.5%, 56.7%, 75.6%, and 44.4%, respectively, for standard images. These values were 63.0%, 72.5%, 66.5%, 80.1%, and 53.7%, respectively, for DES images (Table 4). On DES images, sensitivity, accuracy, and NPV were significantly improved.

Representative cases are shown in Figs. 3 and 4.

DISCUSSION

As lung cancer is now the primary cause of cancer-related deaths world-wide, its early detection and diagnosis are important for improving the survival rate. Chest radiography is currently the most frequently used screening procedure for lung cancer because it is economical and easy to use. However, the false-negative rate for the detection of pulmonary nodules is as high as 19 - 73% for conventional chest radiography^{1,2} and the detection of small lung cancers is especially difficult.⁴ This is partly due to masking of the soft tissue lesion by the superposition of bony structures.

The significant improvement in the detection of pulmonary nodules by adding DES images in our study is supported by earlier investigations that evaluated DES methods at computed radiography or on film-screen systems.¹² Few earlier studies evaluated the performance of radiologists in the detection of pulmonary nodules using DES techniques with the FPD system and the usefulness of this technique with the FPD system has not been established. Tagashira et al.¹³ studied 50 patients with one or more nodules and 50 patients without nodules; they reported that the AUC values of 7 observers were significantly increased from 0.79 to 0.84 with DES images. Ricke et al.¹⁴ evaluated 20 patients with a total of 59 pulmonary nodules; they found that the DES technique significantly improved the sensitivity (from 33 to 42%), specificity

(from 81 to 85%), and confidence in the detection of small pulmonary nodules. On the other hand, Rühl et al.¹⁵ who studied 100 patients with a total of 149 pulmonary nodules (3 - 45 mm, median 11 mm) concluded that at FPD chest radiography, the DES technique did not significantly improve the detection of pulmonary nodules. However, they did not analyze the relationship between nodule detectability and nodule location in the thorax. Our study is the first to investigate the detection of pulmonary nodules from the viewpoint of their relationship to bony structures and nodule density using a DES technique with a FPD radiography system.

Our results suggested that the combined evaluation of DES images and original chest radiographs significantly improved the diagnostic performance of observers in the detection of small pulmonary nodules. The discrepancy between our findings and those of Rühl et al. may be explained by the inclusion of nodules measuring 20 mm or more in their study, suggesting that the DES technique may not improve the detection of large pulmonary nodules that are fully detectable on standard images only. The DES technique may be useful for the detection of small pulmonary nodules.

Our subgroup analysis showed that the improvement in detectability was statistically significant for nodules overlapping with bones; it was not significant for non-overlapping nodules, suggesting that the DES technique may reduce the incidence

of false-negatives by detecting pulmonary nodules that overlap with bones. Our results also suggest that the DES technique yields a statistically significant improvement in the detectability of part-solid nodules, but not of non-solid- and solid nodules. The subtlety of non-solid nodules on images acquired without and with the DES technique may render their detection difficult. For the detection of non-solid nodules, low-dose helical CT may be superior although the clinical significance of the detection of non-solid pulmonary nodules remains controversial. The DES technique was also not helpful for the detection of small solid nodules. Ide et al.⁷ who studied 77 consecutive lung cancer patients and 77 healthy subjects reported that at computed radiography the DES technique failed to improve the detection of non-solid- and solid nodules, however, it significantly improved the detection of part-solid nodules. We posit that conventional chest radiography may yield sufficient detection performance for solid nodules and that the DES technique is useful for detecting part-solid nodules. The malignancy rate of part-solid- is much higher than of non-solid- and solid nodules; it was reported as 63% and 18% for part-solid- and non-solid nodules, respectively.¹⁰ The prognosis is worse for lung cancer patients showing part-solid nodules on CT scans than for those with non-solid nodules,¹⁶ indicating that an increase in the proportion of solid components within a GGO nodule reduces the tumor doubling time, increases the rate of lymph node

metastases and vascular invasion as well as the risk of recurrence.¹⁶ Therefore, it is clinically valuable to detect part-solid nodules using the DES technique.

FPD radiography systems are now widely used because of the rapid accessibility of images, improved image quality, and the possibility of reduced radiation exposure.⁹ The FDP radiography system yields higher detective quantum efficiency (DQE) than computed radiography and film-screen radiography systems.¹⁷ A higher DQE increases the ability to reveal objects in a noisy background¹⁷ and reduces the radiation exposure without sacrificing image quality. At approximately 50% of the radiation dose, the quality of images obtained with the FPD radiography system was equal to that of computed- or film-screen radiography systems¹⁸ and use of the double-exposure technique with FPD may not increase the radiation dose compared with these other systems.

Currently, single- and double-exposure dual-energy systems are available. In the former, DES images are obtained by exposing two storage phosphor plates separated by a copper filter. A disadvantage is the lower signal-to-noise ratio of the tissue-selective subtraction image. Also, theoretically, single-exposure systems cannot be used with FPD systems. On the other hand, in double-exposure systems⁸, two sequential radiographs are obtained at low- and high kV settings, respectively. The

200-millisecond delay between the two exposures may produce misregistration artifacts on the subtracted images. However, double-exposure systems produce DES images with a better signal-to-noise ratio than single-exposure systems.

The massive-training artificial neural network (MTANN) technique is a nonlinear pattern-recognition technique. Suzuki et al.¹⁹ developed a novel method that achieves rib suppression on chest radiographs by using a MTANN. It can produce virtual DES images such as soft-tissue- and bone images from a single chest image obtained with a standard radiography system. As only software is needed, it requires no specialized equipment and no additional radiation dose exposure. We reported that the MTANN technique significantly improved the diagnostic performance of radiologists in the detection of pulmonary nodules.²⁰ We are in the process of comparing the efficacy of the MTANN- and the dual energy technique.

There are several limitations in our study. First, it included a relatively small number of patients; the DES technique should be rigorously evaluated by large-scale clinical studies. Second, we did not evaluate the observers' experience with the interpretation of chest radiographs. Chest radiography is the most common diagnostic tool of radiologists regardless of their years of experience. It may be necessary to clarify the usefulness of the DES technique among observers with different levels of

experience. Finally, we did not evaluate the effect of this technique on the efficacy of detecting pulmonary nodules with calcification. However, calcified nodules can be detected easily on standard- or bone images. Since most calcified nodules are benign, their detection may be of lower clinical significance.

In conclusion, the DES technique combined with the inspection of original chest radiographs significantly improved diagnostic performance in the detection of small pulmonary nodules. We suggest that the DES technique with FPD chest radiography can reduce the number of lung nodules that are missed in routine clinical practice. We recommend that this technique be used routinely to obtain maximum benefits.

REFERENCES

- [1] Kaneko M, Eguchi K, Ohmatsu H, et al. Peripheral lung cancer: Screening and detection with low-dose spiral CT versus radiography. *Radiology* 1996;201(3):798-802.
- [2] Quekel LG, Kessels AG, Goei R, van Engelshoven JM. Miss rate of lung cancer on the chest radiograph in clinical practice. *Chest* 1999;115(3):720-4.
- [3] Sone S, Takashima S, Li F, et al. Mass screening for lung cancer with mobile spiral computed tomography scanner. *Lancet* 1998;351(9111):1242-5.
- [4] Woodring JH. Pitfalls in the radiologic diagnosis of lung cancer. *AJR* 1990;154(6):1165-75.
- [5] Tsubamoto M, Kuriyama K, Kido S, et al. Detection of lung cancer on chest radiographs: Analysis on the basis of size and extent of ground-glass opacity at thin-section CT. *Radiology* 2002;224(1):139-44.
- [6] Shah PK, Austin JH, White CS, et al. Missed non-small cell lung cancer: Radiographic findings of potentially resectable lesions evident only in retrospect. *Radiology* 2003;226(1):235-41.

- [7] Ide K, Mogami H, Murakami T, Yasuhara Y, Miyagawa M, Mochizuki T. Detection of lung cancer using single-exposure dual-energy subtraction chest radiography. *Radiation Medicine* 2007;25(5):195-201.
- [8] Uemura M, Miyagawa M, Yasuhara Y, et al. Clinical evaluation of pulmonary nodules with dual-exposure dual-energy subtraction chest radiography. *Radiation Medicine* 2005;23(6):391-7.
- [9] Bacher K, SmeFPDets P, Bonnarens K, De Hauwere A, Verstraete K, Thierens H. Dose reduction in patients undergoing chest imaging: Digital amorphous silicon flat-panel detector radiography versus conventional film-screen radiography and phosphor-based computed radiography. *AJR* 2003;181(4):923-9.
- [10] Henschke CI, Yankelevitz DF, Mirtcheva R, McGuinness G, McCauley D, Miettinen OS. CT screening for lung cancer: Frequency and significance of part-solid and nonsolid nodules. *AJR* 2002;178(5):1053-7.
- [11] Metz CE, Herman BA, Shen JH. Maximum likelihood estimation of receiver operating characteristic (ROC) curves from continuously-distributed data. *Stat Med* 1998;17(9):1033-53.

- [12] Kelcz F, Zink FE, Pepler WW, Kruger DG, Ergun DL, Mistretta CA. Conventional chest radiography vs dual-energy computed radiography in the detection and characterization of pulmonary nodules. *AJR* 1994;162(2):271-8.
- [13] Tagashira H, Arakawa K, Yoshimoto M, Mochizuki T, Murase K. Detectability of lung nodules using flat panel detector with dual energy subtraction by two shot method: Evaluation by ROC method. *Eur J Radiol* 2007;64(2):279-84.
- [14] Ricke J, Fischbach F, Freund T, et al. Clinical results of CsI-detector-based dual-exposure dual energy in chest radiography. *European Radiology* 2003;13(12):2577-82.
- [15] Ruhl R, Wozniak MM, Werk M, et al. CsI-detector-based dual-exposure dual energy in chest radiography for lung nodule detection: Results of an international multicenter trial. *European Radiology* 2008;18(9):1831-9.
- [16] Noguchi M, Morikawa A, Kawasaki M, et al. Small adenocarcinoma of the lung. Histologic characteristics and prognosis. *Cancer* 1995;75(12):2844-52.
- [17] Floyd CE, Jr., Warp RJ, Dobbins JT, 3rd, et al. Imaging characteristics of an amorphous silicon flat-panel detector for digital chest radiography. *Radiology* 2001;218(3):683-8.

- [18] Hamer OW, Volk M, Zorger Z, Feuerbach S, Strotzer M. Amorphous silicon, flat-panel, x-ray detector versus storage phosphor-based computed radiography: Contrast-detail phantom study at different tube voltages and detector entrance doses. *Investigative Radiology* 2003;38(4):212-20.
- [19] Suzuki K, Abe H, MacMahon H, Doi K. Image-processing technique for suppressing ribs in chest radiographs by means of massive training artificial neural network (MTANN). *IEEE Transactions on Medical Imaging* 2006;25(4):406-16.
- [20] Seitaro Oda, Kazuo Awai, Kenji Suzuki, et al. Detection of small pulmonary nodules on chest radiographs: Effect of rib suppression by a massive training artificial neural network (MTANN) technique on the performance of radiologists. *AJR* 2009 (in-press).

TABLE

Observer	AUC value	
	Without DES images	With DES images
1	0.591	0.625
2	0.633	0.641
3	0.546	0.598
4	0.589	0.734
5	0.68	0.685
6	0.690	0.709
7	0.625	0.739
8	0.605	0.698
Mean \pm SD	0.620 \pm 0.048	0.679 \pm 0.052

Table 1: AUC values for all observers for the detection of pulmonary nodules without and with DES images

Nodule type	AUC value		p value
	Without DES images	With DES images	
Non-solid nodule	0.617 ± 0.101	0.608 ± 0.093	0.725
Part-solid nodule	0.611 ± 0.068	0.689 ± 0.053	< 0.001
Solid nodule	0.750 ± 0.098	0.781 ± 0.078	0.225

Table 2: AUC values for each nodule type without and with DES images

Nodule location	AUC value		p value
	Without DES images	With DES images	
With overlapping by bone shadows	0.664 ± 0.051	0.721 ± 0.054	0.025
Without overlapping	0.584 ± 0.055	0.617 ± 0.055	0.255

Table 3: AUC values for nodule location without and with DES images

	Sensitivity (%)	Specificity (%)	Accuracy (%)	PPV (%)	NPV (%)
Standard image	47.6	72.5	56.7	75.6	44.4
DES image	63.0	72.5	66.5	80.1	53.7
	p < 0.01	p = 0.89	p = 0.02	p = 0.12	p = 0.02

Table 4: Results for nodule detection for all observers without and with DES images

FIGURE LEGENDS

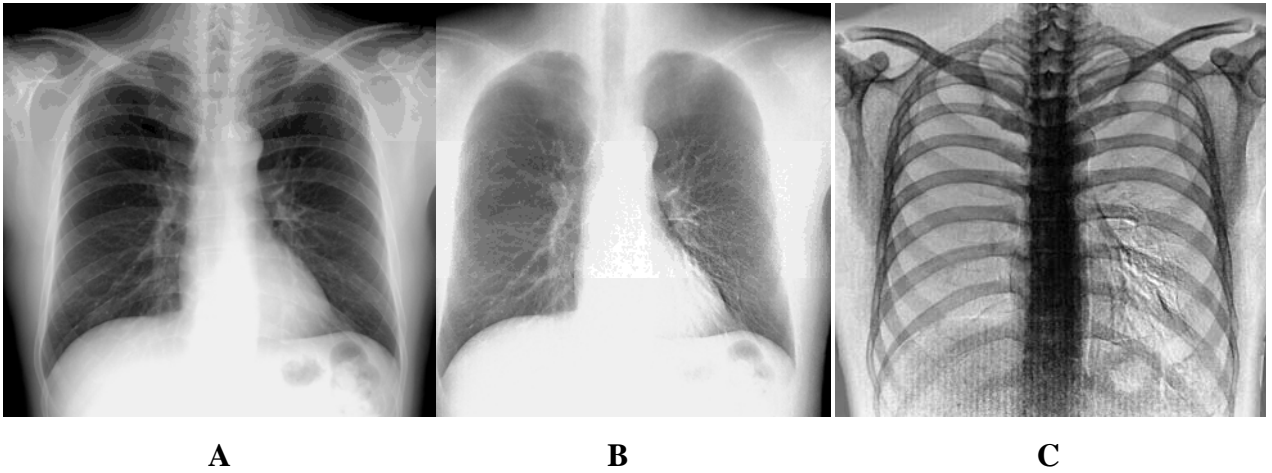


Fig. 1 - Row images obtained at low- and high kVp processed with the DES technique generated the standard posteroanterior image (A), the soft-tissue image (B), and the bone image (C).

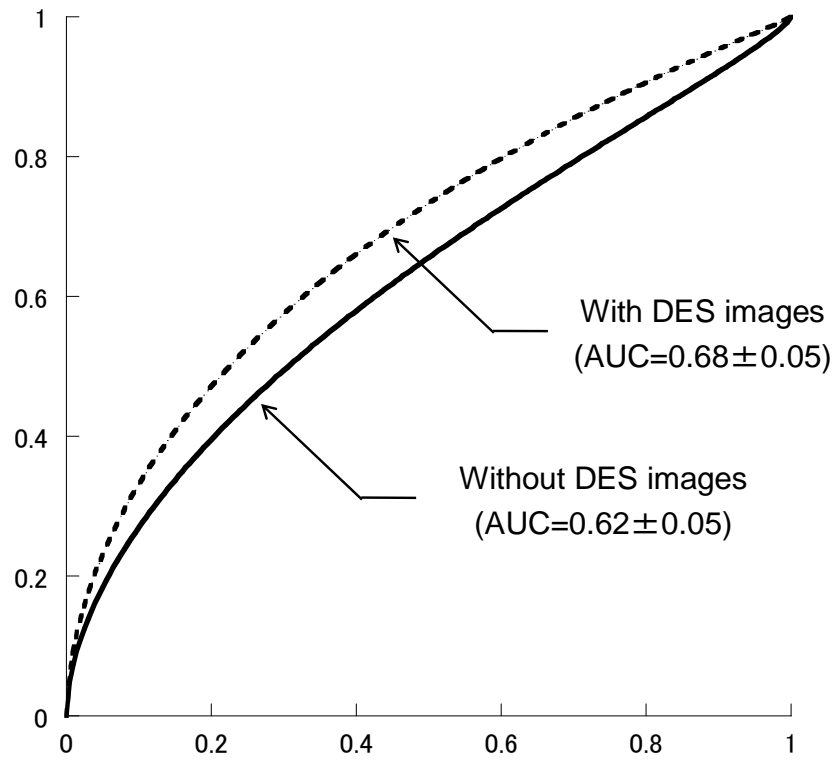
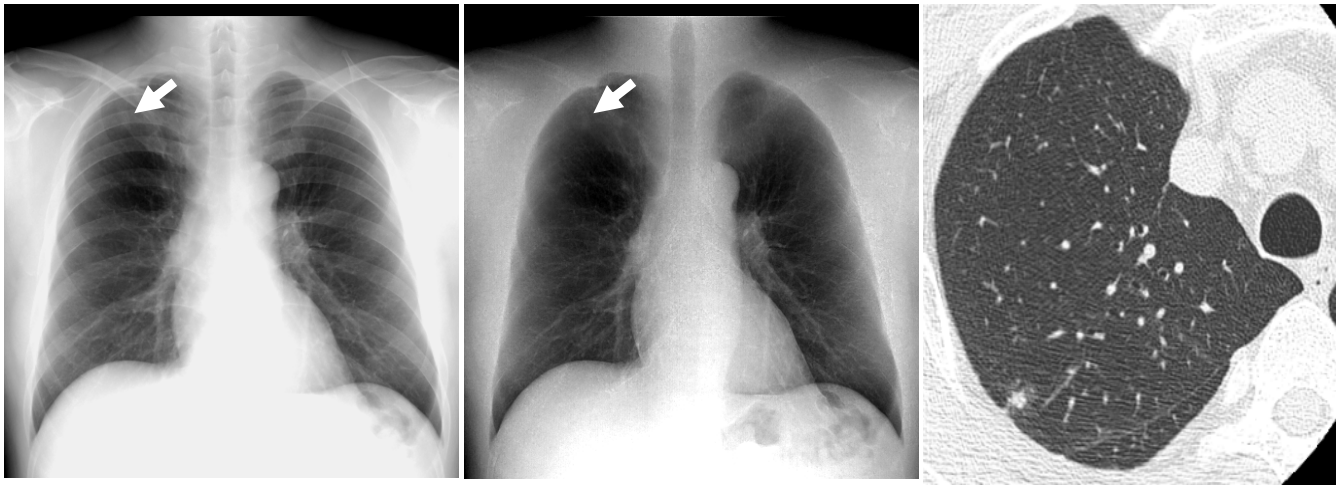


Fig. 2 - ROC curves of the diagnostic performance of all observers without and with DES images. The average AUC value is significantly improved with DES images ($p = 0.02$).



A

B

C

Fig. 3 - Representative case with a nodule.

- A. Standard chest radiograph. There is a small nodule overlapping the rib shadow in the right upper lung field (arrow).
- B. Soft-tissue image produced with the DES technique. The nodule is seen more clearly on the DES image.
- C. CT scan shows a part-solid nodule that proved to be well-differentiated adenocarcinoma in the right upper lobe.

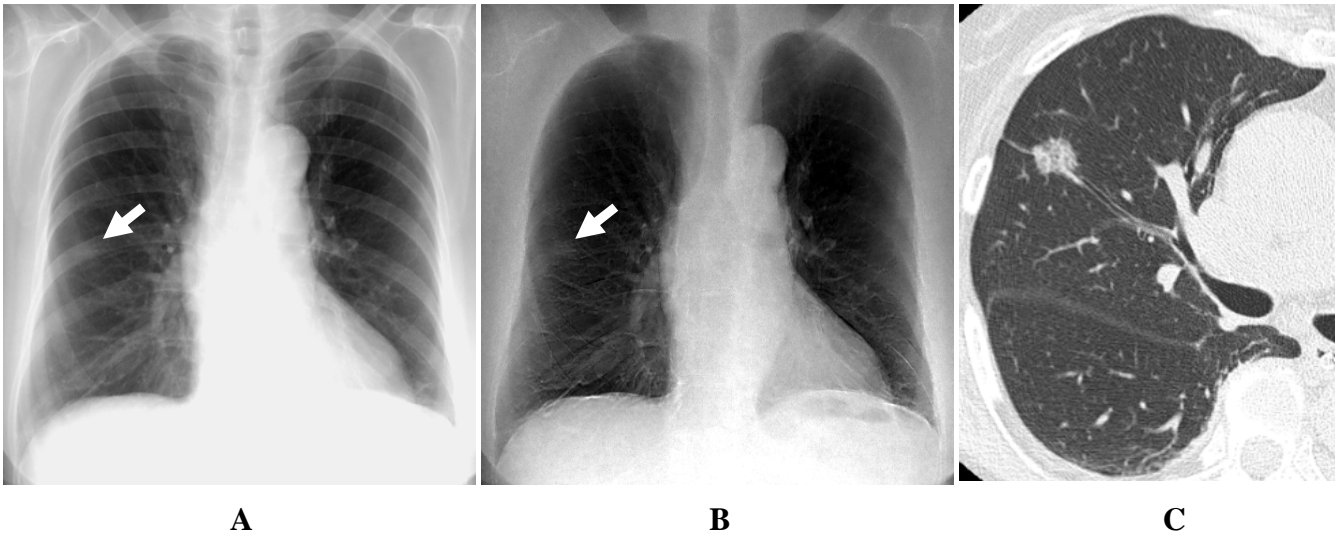


Fig. 4 - Representative case with a nodule.

- A. Standard chest radiograph. Note the subtle nodule overlapping the rib shadows in the right middle lung field (arrow).
- B. Soft-tissue image produced with the DES technique. The visibility of the nodule is maintained on the processed image.
- C. CT scan shows a non-solid nodule that proved to be bronchioloalveolar carcinoma in the right middle lobe.